PhD THESIS

ZSÓFIA VARGA

BUDAPEST

2022

Hungarian University of Agriculture and Life Sciences

Development opportunities for field remote sensing and non-destructive testing of plants

DOI: 10.54598/003350

Zsófia Varga

Budapest

2022

About the Doctoral School:

Name: Doctoral School of Horticultural Sciences

Scientific branches: Agriculture and Horticulture

Head of School: Dr. Éva Németh Zámboriné
Professor, DSc
MATE, Institute of Horticulture,
Department of Medicinal and Aromatic Plants

Supervisors: Dr. András Jung
habil. Associate Professor, PhD
ELTE IK, Institute of Cartography and Geoinformatics

....

Head of Doctoral School Supervisor

I. BACKGROUND AND OBJECTIVES

With the development of remote sensing sensors, spectral and spatial resolution are gradually improving with decreasing sensor size, allowing for the versatile development of remote sensing methods in the field. The results can be directly used in crop protection and nutrient supply research areas related to precision farming and can be linked to the developments of Agriculture 5.0, such as technologies supporting self-driving and autonomous operations, decision support interventions, or embedded systems for automation.

Research into technical solutions based on spectral data can help horticultural field and greenhouse practice. New technical devices such as controllable LED systems have raised awareness of the importance of light-related plant biology research. The possibility of spectral control of light requires a consistent methodology and approach to describing light, while practical approaches use many different systems and metrics, and do not focus on the light requirements of the plant.

The most frequently used tool for field remote sensing is the spectroradiometer. During the development of measurement methods, integration into automated systems gradually comes to the fore. In addition to spectroradiometers, the increasing data collection demand of these systems is supported by new remote sensing device carriers, including drones. As a result, it is possible to collect continuous monitoring data even on a daily basis from an increasingly large area.

The inclusion of spectral data in decision support systems is a gradually increasing global demand. To this end, the primary task is to achieve near-real-time data processing. The increasing sensor resolution, fast data recording, and multi-sensor detection generate an ever-increasing amount of data, which opens up new areas of development in relation to data processing.

In my dissertation, I deal with the investigation of technical developments based on the data collection methods of the spectroradiometer, comparing the accuracy of spectral data collection with the solutions of different sensors, as well as the more frequently used algorithms of spectral data processing during near-real-time interventions.

My scientific objectives are:

1. My goal is to develop prototypes of devices that supplement the measurement methodology with a spectroradiometer, and to evaluate the accuracy of two commercially available spectroradiometers in addition to their application.
2. My aim is to examine whether spectral data can replace field SPAD measurements of chlorophyll content in lettuce (*Lactuca sativa L.*) with sufficient accuracy.
3. My goal is to explore the discrepancies between currently used global irradiance measurement, lux metering and PAR measurement to support the control of new LED lighting systems, and to create a plant-sensing-centric control panel for optimizing light parameters that supports data-driven programming.
4. My aim is to compare correlations and indices between spectral data and water and nitrogen content parameters, and to create a control board to support the automation of this.
5. My goal is to compare the spectral accuracy and intra-day variation of multispectral camera results from drones with the spectral accuracy and intra-day variation of results from a spectroradiometer.
6. My aim is to compare the spectral accuracy of multispectral camera results from drones with the spectral accuracy of satellite remote sensing.
7. My goal is to determine the accuracy and run-time of spectral image processing algorithms for near real-time data processing.

II. MATERIAL AND METHODS

2.1. Support for field measurement methodology for passive field spectroradiometers

2.1.1. Design and construction of prototype clip-on measuring head and stand

I designed an adjustable tripod system based on the dimensions of the Qmini spectroradiometer to help keep the sensor at fixed distances and angles in the field. The tripod consists of a sensor holder design that holds the sensor at a 45 degree angle. The sensor holder is capable of 360 degrees of rotation and can be slidably mounted at different heights on two sizes of rod attached to a base for stability.

I designed a hemispherical gauge head in *AUTOCAD 2021* software, and then fabricated it with *Creality Ender 3D* printer using ABS filament material. I coated the

measuring field of the measuring head with barium sulphate paint. I used a microscope lamp with G4 socket as light source, the socket of which can be fixed on the outside of the measuring head. As power source I connected a Parrot drone lithium-polymer battery and a circuit breaker switch. To connect the sensor, I designed 2 inputs, one for transmittance measurements facing the light source at 180 degrees and the other on the side of the light source at 45 degrees.

2.1.2. Comparative measurements of spectroradiometers

The measurements were carried out in the summer of 2017 in the wine region of Hajós-Baja, in Borota, in the Koch Winery. 100 samples at the same point, taken consecutively with two spectroradiometer systems (*ASD Fieldspec2* spectroradiometer with *Plant Probe*; *Qmini* spectroradiometer with prototype probe). Statistical evaluation was performed by one-factor analysis of variance (*Excel*) after condition testing, comparing the accuracy of the two systems. In addition, I examined the REP (Red Edge Point) values that were typical during the measurements, since this point is the basis of several spectral indices. I characterized the evaluations by the mean and the percentage variation of the deviations of the values for easier comparison.

2.2. Studies in different lighting environments

2.2.1. Comparative measurements with Konica Minolta SPAD 502 measuring system

For the chlorophyll study, I set up three growing tents with 20-20-20 lettuce plants (*Lactuca sativa L.*) per tent. The experimental environment was set up by growing in artificial rockwool cubes, providing the same nutrient solution concentration, keeping climatic parameters constant, and setting the same lighting length. The only difference was in the illumination, so in two tents I used high power LED systems (a *KIND LED K5* panel and a *Tungsram Research Module* at 50% power), while in the third case I used a HPS system (*Sylvania SHP-T Growpress* 600W).

For the SPAD measurements I used the *Konica Minolta 502* SPAD device of the Hungarian University of Agricultural and Life Sciences, Institute of Horticulture, Department of Vegetable and Mushroom Production. I measured 3-3 leaves per

lettuce plant, with both sensor systems in three replicates. The final result was 58 measurements per tent. A total of 174 averaged data were obtained for the three tents, of which 165 were analysed in further analysis). The total chlorophyll content of the leaves analysed was quantified spectrophotometrically at specific wavelengths after acetone extraction. After extraction, the filtrate was loaded into glass cuvettes and absorbance was measured against the acetone blank sample at λ=661.6; λ=644.8; λ=470nm using a Helios-alpha spectrophotometer. Calculation: Cl_a (μg/mg) = 11,24*A661.6 - 2,04*A644.8, Cl_b (μg/mg) = 20,13* A644.8 - 4,19*A661.6, C(x+c) (μg/mg) = (1000*A470-1,90*C_a-63,14*C_b)/214. The chlorophyll content determined by analytical measurements was compared with the SPAD values and the results of the spectral indices calculated from the measured data, using a paired t-test.

2.2.2. Creation of a control panel for the control of lighting systems and the input of light parameters from spectral data

In my work, I have presented the technical approaches of global irradiance pyranometers, quantum sensors measuring the PAR range, and luminometers measuring the illuminance of light, the sensitivity of the measurement systems used in practice, and the characteristics of the photometric parameters that can be associated with a given solution.

Starting from the solar irradiance data described in Gueymard's 2004 paper, I combined the physical equations in a model, which extended from Planck's law to the photometric equations. Since my particular measurement system uses the photopic vision (V(λ)) curve as recorded in *CIE S010/E:2004*, I have corrected the corresponding values in the model. I also processed the measurement sensitivity characteristics of the different measurement systems. Based on these, I have presented the differences.

The model equations have been improved so that the table automatically recalculates and plots the actual photometric parameters based on any spectral measurement. Also, as a new element, it weights the spectral results based on the absorption curves a and b of chlorophyll. In addition, the photon flux is given for the PAR range 380-700 nm and 380-750 nm. In its final table, it compares the measured results with a reference spectrum, showing the differences by wavelength.

I demonstrated the operation of the control panel by measuring several lighting systems. At the same time, the evolution of the photometric parameters of two high-power LED systems (*KIND LED K5 panel* and *Tungsram Research Module*), a lighting system in a phytotron (*SANYO*), an HPS system (*Sylvania*) and the spectral data of the Sun were measured.

2.2.3. Analysis of content parameters based on spectral values

2.2.3.1. Spectroradiometric detection of plant water stress

To evaluate the water stress detection of remote sensing indices and spectral data, two plant growing tents were set up, and unlike before, the light source (*Tungsram Research Module*) was of the same design. In the tents, I grew pepper (*Capsicum annum L.*) plants on rockwool cubes with 25-25 plants per tent. I applied the same amount of irrigation for the first month in both tents and nutrient solution application starting from the second week. From the second month onwards, I halved the watering of the plants in the second tent.

After one month, I performed the spectral measurements in triplicate using the prototype measuring head. Then, in an analytical laboratory, I measured the relative water content of the leaves examined and compared these values with the spectral data. The correlation of several spectral water indices with the analytical test results was investigated.

2.2.3.2. Detection of plant nitrogen supply by spectroradiometer

Similar to the previous approach, I set up two separate growing tents using the same LED light source. I grew basil (*Ocimum basilicum L.*) and lettuce (*Lactuca sativa L.*), 25-25 seedlings of each species, on rockwool cubes.

I used 5 treatments to test nitrogen application. I pre-determined the appropriate amount of nutrient solution for each species, and then developed a "dilution series" with a 5 mg rate so that the plants in sample number 3 received the optimum amount, samples 1 and 2 received 10 and 5 mg less, while samples 4 and 5 received 5 and 10 mg more from week 2 onwards. In this way, I investigated the correlation of the spectral indices with nitrogen by establishing different nitrogen dosages.

Spectral measurements were taken in the first month after the start of treatment, with three replicates of three sample leaves on each plant. The nitrogen content as a percentage of dry matter was measured in an analytical laboratory and compared with the spectral indices.

2.2.3.3. Developing solutions for spectral index data processing

Since spectral indices help many remote sensing data processing, simplifying large data sets from an automation point of view, but can be time-consuming to calculate, I created two auxiliary files to speed up the process of defining spectral indices for later analysis.

In one direction, for field spectroradiometer measurements, I created a spreadsheet that automatically gives the major water indices, the major nitrogen indices, the chlorophyll indices seen earlier, and produces the first-order derivatives of the spectral data, calculating the minimum and maximum values of the RedEdge range, inflection point and slope from the readings in subsequent worksheets. Where analytical measurements are available, I have also developed a worksheet for inputting these data, using each pair of worksheets to examine the correlation of the indices and to provide the values for the underlying statistics. It calculates and, where appropriate, correlates over 50 spectral indices simultaneously.

As a solution to help processing the image data, I created a *JavaScript* code to use the open source system of *QGIS*, which is copied to the appropriate local library and incorporated into the program's 'Raster calculator' algorithm. When used, it displays all the indexes in a drop-down menu for the user, then gets the required channels and generates the layer according to the requested index without any other operation. I have included a total of 40 spectral indices, so that others can speed up this processing step.

2.3. Comparison and data processing assessment of multispectral sensors on new UAVs

I have conducted a comparative analysis of the remote sensing accuracy of multispectral cameras carried on new launch vehicles (*UAVs*), comparing both the accuracy of satellite remote sensing and the results of spectroradiometer measurements.

2.3.1. Comparison of multispectral camera measurements on drones with spectroradiometer measurements

For comparison with spectroradiometer measurements, I used raw data from the Harvard Dataverse Wageningen University measurement database. From this database, I compared the *Sequoia* camera files with the reflectance measurement results of two commercially available spectroradiometers (*Cropscan, Tec5 Handyspec*). Measurements were taken at the same time of day between 7:25 am and 8:00 pm at 9 different times, recording two potato fields, two wheat fields, one barley field, the open soil surface, and calibration plates of different sizes at several locations. All measurements were taken simultaneously with both spectroradiometers, and the *Sequoia* multispectral camera carried on the drone.

Since, from a remote sensing point of view, multispectral cameras used on drones perform less calibration in practice, it is particularly important to compare the two methodologies in terms of accuracy.

The raw data was pre-processed, reflectance values were extracted from the image file for each measurement point, and then variance analysis was performed on a channel-by-channel basis to investigate the differences, comparing the possible effects of time of day on accuracy.

2.3.2. Comparison of multispectral camera measurements from drones with satellite remote sensing measurements

For the study, I used measurements from a *Micasense Altum* six-channel multispectral camera. The measurement was carried out on 08.09.2021 with a *DJI Matrice 210 RTK* drone in the sportfishing area of Lake Tisza. The total surveyed area was 25.5 ha, the measurement was performed at an altitude of 70 m and the resulting images had a spatial resolution of 1.6 cm (GSD = 1.6 cm).

For comparison with satellite remote sensing, Sentinel-2 MSI2A satellite images of the same area at the same time were processed. Alternatively, since *Micasense Altum* also records a thermal channel, I included a *Landsat-8* satellite thermal image for the purpose of this analysis. Both satellite images and *Micasense Altum* images were pre-processed, and after loading the same areas and running the

supervised image classification algorithms, the results were examined and compared using accuracy assessment.

For the purpose of analysing spectral data, I have assigned 150 points in the field, with 25-25 points within each class. For the matched channels, I collected the measured reflectance values for these, averaged them by class and analysed the variance.

2.3.3. Evaluation of image processing algorithms for near real-time data processing

The characteristics of the data set acquired with *Micasense Altum* presented in the previous section are: 6 x 940 images, 6 x 1.56 GB single-channel orthomosaic images after pre-processing, 10 GB as 6-channel stacked images, 8 GB for the 5-channel stacked version, the resulting file size containing more than 620 million pixels of data points per channel.

After pre-processing this data file, I tested the following image classification methods by running them on the 5-channel image. The unsupervised clustering (using ISODATA method), the minimum distance (MD), maximum likelihood (ML) and spectral angle mapper (SAM) algorithms among the supervised image classification, the Random Forest (RF), Artificial Neural Network (ANN) and Support Vector Machine (SVM) models among the machine learning solutions, and the Convolutional Neural Network (CNN) model for deep learning.

For the near real-time automation solution, I have developed two machine configurations with a 4 GB and an 8 GB DRAM capacity, as these are the closest to the microcomputer units used in the automation. I have run the algorithms in parallel, testing their runtimes. For accuracy assessment, I created a reference layer based on the field survey, comparing the overall accuracy in percentage, the Kappa index value, and the area ratio of correct and incorrect pixels by cross-classification.

In addition to the algorithms listed above, I investigated the possibility of PCA analysis, its running characteristics and accuracy. Also, a Python-based decision tree design was used to run the classification.

The examined classes of vegetation cover were: class 1.- water chestnut (*Trapa natans*), class 2.- common reed (*Phragmites australis*), class 3.- cattail (*Typha*

angustifolia), class 4.- water surface, class 5.- fairy rose (*Nymphaea alba*) and class 6.- sedge (*Carex acutiformis*). For training I used 60% of the reference layer for validation. For the analysis I used the *SCP* and *ORFEO* plug-ins of the *QGIS* software.

III. RESULTS

3.1. Field application development results and comparative results

3.1.1. The final version of the prototype

The prototype probe head converts our instrument into an active sensor to speed up field measurements. The hemispherical design of the probe combines approaches from diffuse spectroscopy. No similar design is currently available on the market.

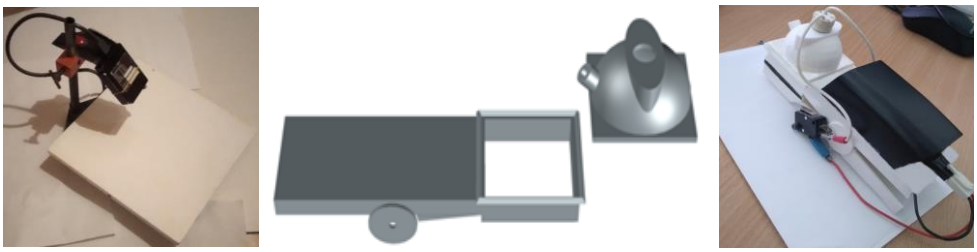

Figure 1. – Picture of designed prototypes, left the measuring stand, middle the model of the measuring head, right the improved model

With the stand, we can measure at a fixed angle of 45°, with 360° adjustable rotation, at a registerable and adjustable height. In the final prototype version, the measuring head has been fitted with a support to make it easier to fix the light source. By making the measuring head interchangeable, it can be further developed in a variety of other configurations (for example, for testing berry crops). Once the technical model is available, it can be reproduced and further developed by anyone.

3.1.2. Comparative measurements with ASD Fieldspec 2 Plant Probe measuring system

The difference in the REP (Red Edge Point) values for the measurements is summarised in Table 1.

Table 1. - Summary comparison of ASD Fieldspec 2 and Qmini measurements for REP

REP average - prototype (nm)	Average standard deviation	**Deviations as a percentage of the REP average (%):**
718,005	1,118	**0,156**
REP average - ASD (nm)		
718,156		

The results show that the two instrumental solutions are a good substitute for each other. Accordingly, the clip designed and manufactured by us has sufficient accuracy for field testing.

3.2. Results of tests in different lighting environments

3.2.1. Results of comparative measurements with the Konica Minolta SPAD 502 measuring system

Table 2. - Statistical comparison of chlorophyll index values measured with a measuring head and SPAD meter data with laboratory results using a two-sample t-test (extract for correlation and standard deviation results)

	Expected value	Standard deviation	Number of samples	Pearson's correlation	R^2
Chlorophyll a+b	33,85	495,88	165		
CI_{green}	2,39	1,06	165	0,94	0,88
MTCI	0,17	0,02	165	0,99	0,97
MCARI	0,36	0,05	165	-0,83	0,69
NDVI	0,78	0,004	165	0,58	0,33
MCARI	0,63	0,28	165	0,98	0,97
CCI	12,84	165,64	165	0,92	0,85
$CI_{rededge}$	0,15	0,014	165	0,99	0,97
SPAD	32,52	164,59	165	0,96	0,93

Statistical analysis showed a significant (α=0.05) and strong correlation between analytical total chlorophyll content and chlorophyll predictive indices. The best chlorophyll predictor index was found to be the $CI_{rededge}$ index (R=0.99), followed closely by the MTCI (R=0.98) and MCARI (R=0.98). These three indices achieved higher correlations than the values detected by the SPAD meter, i.e. they are more accurate predictors of total chlorophyll. This also demonstrates that spectroradiometer measurements can replace SPAD meters.

3.2.2. Determination of photometric parameters from spectral data

To illustrate the sensitivity of the different systems and their respective weighting solutions, I show the basic differences in the Sun measurement in Figure 2

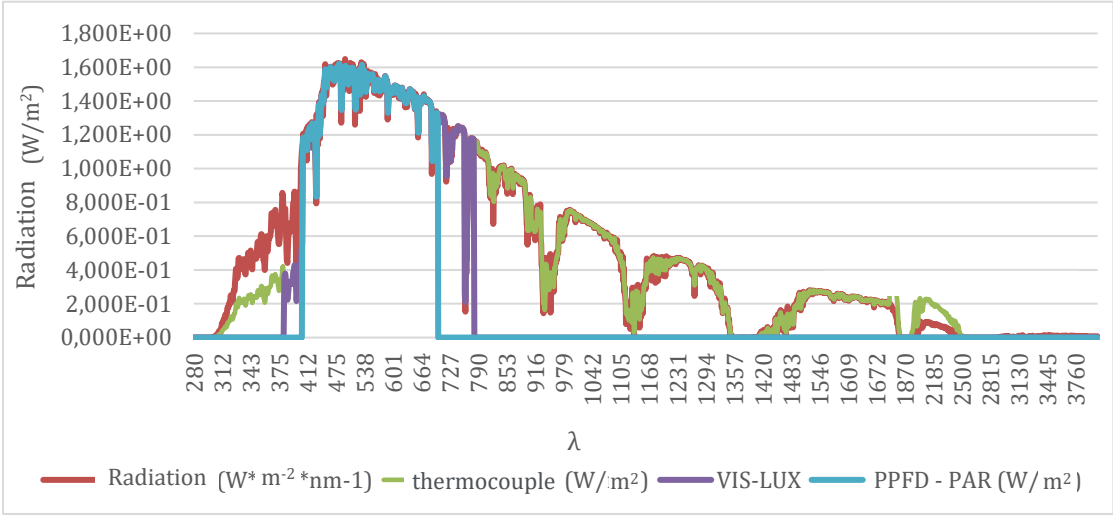

Figure 2. - Different sensor sensitivities modelled on solar measurements

The user can select the measurement resolution. The model gives the maximum wavelength calculated from spectral data, the total irradiance (W/m^2), the PAR PPF photon flux ($\mu mol/m^2/s$), the calculated lux (lm/m^2). Since the photon flux density can only be calculated in situ at a given distance, I used a logarithm approach to replace the calculation of these values, and then weighted by chlorophyll absorption to display the same values. Each calculation is first calculated for an extended range (380-780 nm) and then narrowed down. A picture of the control panel results area is shown in Figure 3.

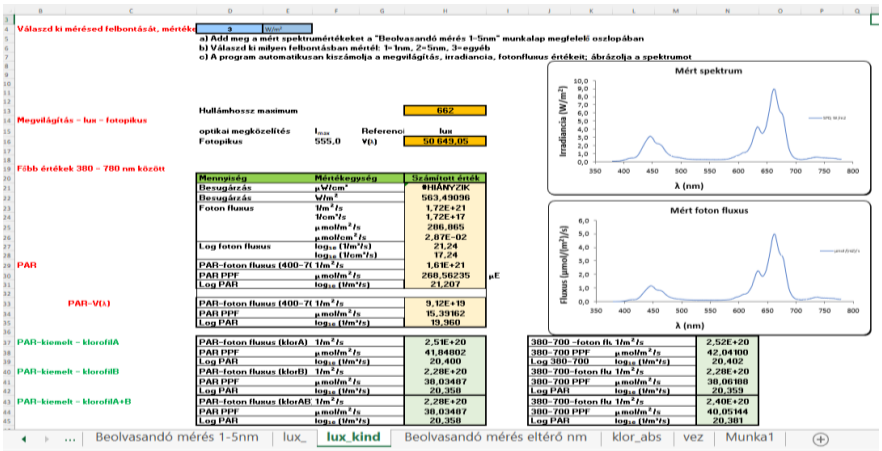

Figure 3. – Image of a scoreboard of photometric parameters calculated from spectral measurements of the KIND K5 high-power LED system

The control panel can help you compare different luminaires. An illustration of this is shown in the following Figure, which shows the chlorophyll absorption-weighted values of four different artificial light sources and the Sun.

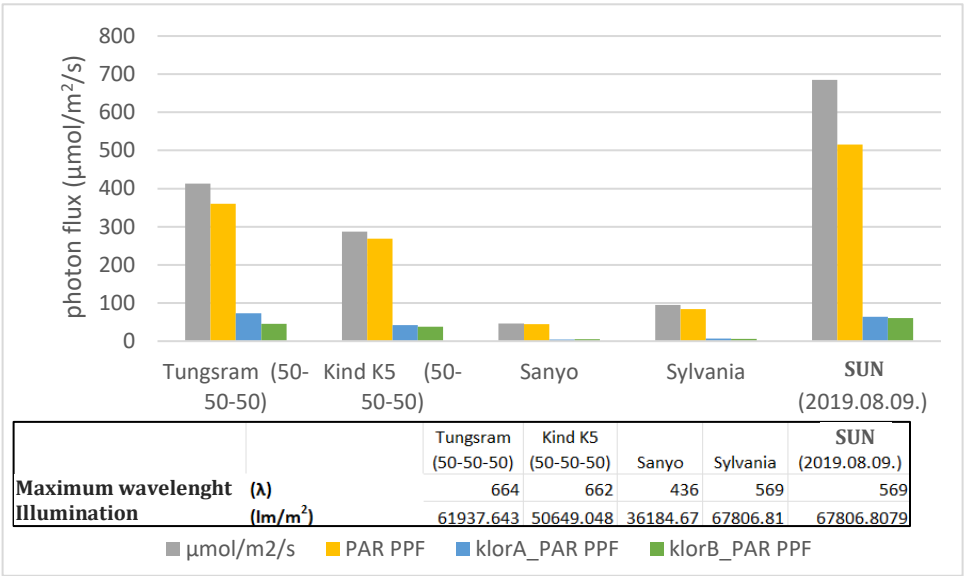

		Tungsram (50-50-50)	Kind K5 (50-50-50)	Sanyo	Sylvania	SUN (2019.08.09.)
Maximum wavelenght	**(λ)**	664	662	436	569	569
Illumination	**(lm/m²)**	61937.643	50649.048	36184.67	67806.81	67806.8079

Figure 4. – Presentation of results calculated from 4 artificial lighting systems and the Sun (09.08.2019)

I have shown with Figure 4 that in some cases a high illumination value (Sylvania), but not even a high PAR PPF value, does not necessarily mean a useful photon composition for the chlorophylls of plants. However, new LED systems can be designed with a choice of the spectral range emitted by the diode, thus creating light sources optimised for plant photoreceptors, in contrast to previous practice. Currently, I have used data from an August solar survey as a reference for the control design. The development of an accurate reference will be very important in the future towards spectrally controlled supplementary lighting controls, where a greenhouse lighting system is used to make up for the missing amounts of natural radiation.

3.2.3. Correlation of water stress with spectral data

A total of 26 different water indices were formed by processing our spectral data using the auxiliary table presented in section 2.2.3.3. The correlation of these indices was compared with the analytical results. The strongest correlations are summarized in the following Table 3.

Table 3. – Summary table of water index values and laboratory moisture correlation results

Indices	R
NDMI	0,91
NDWI	0,91
WI (900/970)	0,79
WI (970/900)	-0,79
MSI	-0,91
LVI2	**0,94**
1200/850	-0,77
1450/850	**-0,92**
1650/850	-0,89
(970-900)/(970+900)	-0,79
(970-850)/(970+850)	-0,57
970-880	-0,8
SRWI(860/1240)	0,68
970-920	-0,87
NDWI(960-1240)	0,69

PLS-R analysis was used to investigate further more sensitive ranges. I also performed this analysis on the values of the first-order derivative (Table 4). I also examined the simple, simple ratio and normalized versions of the most sensitive wavelengths for correlation.

Table 4. – The top 5 indices in a table summarising the correlation of the indices formed by the first-order derivatives of the measured spectral values

Indices	Pearson' correlation (R)
MSI	-0,91
LVI2	**0,94**
1450/850	**-0,92**
1650/850	-0,89
970-920	-0,87

3.2.4. Correlation of nitrogen treatments with spectral data

The results of the PLS-R analysis show that the "more sensitive" wavelengths in the spectrum are at 800, 710, 675, 560 nm. From these ranges, I formed new indices and examined the RedEdge range with a higher focus.

Unfortunately, for none of the indices did the indices show a high significant correlation, only a medium result. The highest correlation value was obtained for the

S800/675 index (R=0.52), followed by the CRI (R=0.49) and the minimum value for the 650-800 nm range (R=-0.48).

3.2 Results of a comparison of multispectral sensors on new Unmanned Aerial Vehicle (UAV) systems

3.2.1. Comparative results of a drone Sequoia multispectral camera and two spectroradiometers

The data show that the two systems can replace each other with reasonable accuracy, with the standard deviation squared differing minimally for most channels, so less calibration of the drone cameras does not necessarily mean a disadvantage in terms of accuracy.

Higher variance was observed in the NIR channel, which showed higher values (~3 and 1.5) both between the two systems and between the multispectral camera intra-day values. This was examined in more detail (Figure 5)

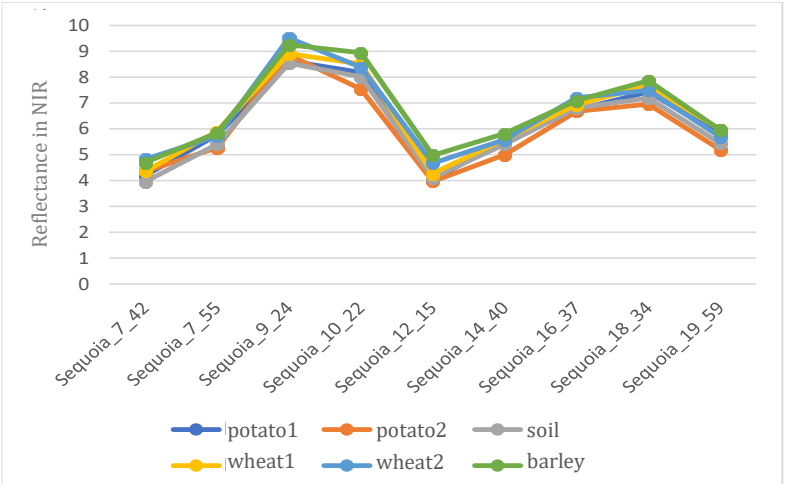

Figure 5. - Reflectance values in the NIR channel measured by Sequoia camera at different times for different surface coverages

It can be seen that the main differences are in the 9:00 a.m. - 10:00 a.m. period and in the afternoon (between 16:30 p.m. - 18:30 p.m.).

3.2.2. Results of the comparison of Micasense Altum images with satellite systems

The optical channels were compared with the Sentinel-2 MSI2A satellite image, while the thermal channel was compared with the Landsat8 thermal image.

Due to the greatly increased spatial resolution of the drone imagery, we can achieve much more detailed imaging and analysis compared to a satellite image. However, the vegetation boundaries are highly coincident.

In terms of accuracy, for 6 classes, Sentinel-2 swapped the smaller class of sedge for the dominant species using the maximum similarity algorithm, while fairy rose became the dominant species using the minimum distance method. The main reason for this is that on the one hand, the eagle owl could be trained with a small area, which is not a difficulty for a detailed (drone) image, but on the other hand, for a less detailed image, it is amplified by the fact that the spectral data for the two classes became too similar, as indicated by the Bray-Curtis similarity analysis (value 92.58% for the two classes). In addition, satellite analysis of the fairy rose is not possible because it was mostly scattered, which cannot be trained with a lower spatial resolution.

With 4 classes, both methods showed good accuracy. Among the algorithms, the spectral angle method achieved the highest accuracy in both cases and for both methods.

The results of the standard deviation squared of the data extracted to test the spectral accuracy against each other showed that the highest value was 0.05, while the average was 0.02.

With the above, I have demonstrated that, in terms of spectral accuracy, the drone-borne remote sensing method can adequately replace satellite imagery analysis, and in addition, for some research areas, satellite remote sensing is no longer an appropriate methodology. Satellite-based systems can be used to monitor changes in land cover over large areas, while drone-borne instruments can be used to monitor changes at the scale of smaller spatial units, and thus for near real-time interventions.

A similar result was obtained when analysing the thermal channel, where the spatial differences became even more pronounced, as the spatial resolution of the Landsat8 satellite image is lower than that of Sentinel-2.

3.1.3. Results of running time and accuracy assessment of different classification algorithms

The results for the two configurations are summarised in Table 6.

Table 6. – Results of image classification algorithm runtimes and Kappa index values for the full model

Image processing algorithms		8GB DRAM	4GB DRAM	Kappa index
		running time (h)		
unsupervised	Clustering (ISODATA)	9.7	>24h	0.4
deep learning	Convolutional neural network (CNN)	>24h	-	0.68
machine learning	Random Forest	7.4	>24h	0.65
	Support Vector Machine (SVM)	10.6	>24h	0.64
	Artificial Neural Network (ANN)	10.2	>24h	0.64
supervised	Minimum Distance (MD)	1.2	6.5	0.52
	Maximum Likelihood (ML)	1.2	6.5	0.6
	Spectral Angle Mapper (SAM)	1.2	6.5	0.65
	Principal Component Analysis (PCA)	3.5	8.5	0.56
	Python based Decision Tree Rules	0.5	2	0.56

The results show that although the deep learning model, followed by machine learning methods, achieved the best results in terms of accuracy, their high running times do not allow for near real-time data processing. In contrast, the spectral angle algorithm has been characterized by an adequate overall model accuracy even at significantly faster run times. At class level accuracy, each algorithm showed results of 80-90%.

The decision rules were designed with 5 unique features for each class using the simple reflectance layers, the PCA results, the NDVI layer and the thermal channel. This method can be easily integrated with any Python environment and can help near real-time development due to its significantly lower runtime. It can also help more complex analyses (e.g. changes in plant density). On the automation side,

the definition of specific rules is not yet solved, as these properties do not necessarily coincide with the basic statistical values (minimum, maximum, average).

IV. DISCUSSION AND CONCLUSIONS

4.1. Development results of spectroradiometer's methodology

In my comparative measurements, I have shown that a spectroradiometer that performs spectral measurements can replace the SPAD meter, the lux and PAR measuring systems used for light measurement, with sufficient accuracy.

The accuracy of the designed measuring head is in line with the solution developed by the most common manufacturer, it also better implements the principle of the measuring system used in the diffuse spectroscopy laboratory and it facilitates further development by means of its interchangeable head. In the future, it is advisable to further investigate the possibility of changing the internal surface coating and using different washers.

The control panels can be easily integrated into data-driven programming using the widely used Visual Basic.

In my comparative measurements, I have shown that by measuring spectral A light parameters with spectral data, we can express all other characteristics. In addition, a change of approach that takes the absorption of plant light receptors more into account than the PAR approach would be important. A light control focusing on the absorption of the photoreceptors and adapting it to the natural illumination can only be achieved with spectral control, so the use of spectroradiometers is proposed from the automation side. It will be important to further research appropriate references, which may vary according to the needs of a particular crop species beyond local conditions.

Another objective of my results on the content (chlorophyll, water content) was to demonstrate that specific spectral indices can adequately replace laboratory destructive measurements. In the future, it will be recommended to reduce the number of these indices, in particular for automation purposes. For example, if, in further measurements, $CI_{rededge}$ predicts chlorophyll with a similarly high value under different plant species and different environmental parameters or stress, this index could be incorporated into technical developments.

The model of the measuring adapter and the two control boards are available to anyone at the link below:
https://drive.google.com/drive/folders/1DuYy_X1CSGoT0tMv85gKHQ9iH0XRmjIw?usp=share_link/

4.2. Investigating new equipment carriers

I have shown that, although multispectral cameras on drones are less calibrated, they can replace spectroradiometer measurements with reasonable accuracy. It will be important to verify this with further studies, involving a larger number of sensors.

Further investigation of the NIR channel will also be important, as many spectral indices are based on this measurement. For the time being, because of the variance observed here, I would recommend that any data collection solution using a drone-carried multispectral camera should be performed during midday.

I have shown that while both satellite and drone systems are accurate when analysing larger spatial units (with fewer classes), satellite systems will not be able to provide accurate analyses when focusing on smaller spatial units. This means that the development of near real-time solutions can also be achieved by including drone-based multispectral sensors.

In terms of near real-time interventions, current data processing directions cannot deliver the required speed for this amount of data. The future solution could be multi-directional:

- A characteristic of deep learning solutions is that the larger the background database of the model being trained, the more training runs we have done, the faster the speed of the runs becomes. For this purpose, the recordings of remote sensing sensors used on drones should be collected in a database (no such database exists yet, only some measurements are available).
- Efforts should be made to use simpler data structures. For example, by using a Python-based decision tree, we can simultaneously include several different layers and thus different data in the analysis. At the same time, it is recommended not to include a multichannel data array, but simpler spectral indices, reflectance values for

a given range, or temperature data. This approach implies the linking of individual properties, so that a future database of these individual properties has to be developed.
- The optimal data size analysis approach: analysis of the image data set in smaller units. The definition of these parameters is something I would like to explore further in the future, which could be aided by, for example, the collection and analysis of *ORFEO* '*log*' data. When running the algorithms, *ORFEO* estimates the computing capacity required for the entire task (in this research, the three machine learning models on such a large dataset required 23800 GB of DRAM), then decomposes the task according to the available memory and executes the task step by step. Thus, a longer-term study of this data can help to design the optimal data set for near real-time improvements.

V. NEW SCIENTIFIC RESULTS

1. I have designed, developed and tested an optical leaf measurement adaptor (clip) with comparative measurements, which has been shown to have good field utility and significantly improves the performance of contact plant spectroradiometric measurements.
2. Developed a standardized data collection and data conversion methodology adapted to spectroradiometers that significantly improves interoperability, transparency and comparability between spectral measurements, especially for SPAD meters, $CI_{rededge}$ indices, Lux and PAR measurement systems, and for chemical laboratory measurements of chlorophyll and water content.
3. I have demonstrated that a drone multispectral camera system can replace field spectroradiometer calibration measurements with satisfactory accuracy when data are collected at or near the maximum solar zenith.
4. I have demonstrated that the drone multispectral camera system can replace the measurements available from satellite remote sensing with greater accuracy, It will be useful to integrate this methodology into the development of more detailed field analyses, and thus near real-time interventions.
5. Developed a near real-time drone image processing technique using traditional and artificial intelligence image classification methods for decision-supporting rapid assessment and anomaly detection.

VI. PUBLICATIONS RELATED TO THE TOPIC OF THE THESIS

1. Journal articles with Impact Factor:

NAGY Á.Z., JUNG A, **VARGA ZS.**, KÁTAY GY., ÁDÁM L.A. (2017): Effect of Artificial Light Conditions on Local and Systemic Resistance Response of Tobacco to TMV Infection; N*otulae botanicae horti agrobotanici Cluj-Napoca,* 45:(1) pp. 270-275. IF=0.575 (2017), *https://doi.org/10.15835/nbha45110751*

VARGA ZS., VÖRÖS F., PÁL M., KOVÁCS B., JUNG A., ELEK I. (2022): Performance and Accuracy Comparisons of Classification Methods and Perspective Solutions for UAV-Based Near-Real-Time "Out of the Lab" Data Processing; *Sensors - Feature Papers in the Remote Sensors Section,* 22*(22),* 8629*;* IF= 5.349 (2021), *https://doi.org/10.3390/s22228629*

2. Peer-reviewed journal (MTA list) publications:

CSIMA GY., **VARGA ZS**., FICZEK G., GYÖKÖS G., LÁNG Z. (2015): Comparison of Fresh Apple Quality grown on Different Tree Trellises, *Hungarian Agricultural Engineering* (27) pp. 51-55., *http://doi.org/10.17676/HAE.2015.27.51*

VARGA ZS., FELFÖLDI J., STEINER M., LÁNG Z. (2015): Study of inlet light spectrum's effect on plants growth - the light transmittance decreased with increasing glass thicknesses, *Hungarian Agricultural Engineering,* (30), pp. 17-22, *http://doi.org/10.17676/HAE.2016.30.17*

SIPOS L., BOROS I., PURCZEL Á., **VARGA ZS.,** SZŐKE A., SZÉKELY G. (2017): LED-ek hasznosítási lehetőségei a növénytermesztésben (review). Kertgazdaság 49(3). pp.11-22

3. Conference full papers:

LÁNG Z., CSORBA L., **VARGA ZS**. (2013): Achieving Constant Amplitude and Acceleration of Shaken Fruit Trees Using An Extended Inertia Shaker Machine, *Synergy International Conference*, Gödöllő, Paper no. 193.

VARGA ZS., JUNG A. (2019): Különböző LED rendszerek üvegházi alkalmazásának hazai tapasztalatai; *X. LED konferencia (2019.02.05.),* pp. 23-24.

VARGA ZS., VÖRÖS F., PÁL M., KOVÁCS B., JUNG A., ELEK I. (2022): Osztályozási módszerek és új megoldások teljesítményének és pontosságának összehasonlítása UAV-alapú, közel valós idejű adatfeldolgozás céljából; *XIII. Térinformatikai Konferencia és Szakkiállítás (2022. 11. 3-4.)*, pp. 325-337.

VARGA ZS., JUNG A. (2016): A spectroscopic set-up development for efficiency analysis of HPS and LED lighting in horticulture; *Biosysfoodeng (2016.12.08.),* Paper no. 136.

4. Conference proceedings (abstracts):

VARGA ZS. (2020): Különböző LED-rendszerek kertészeti alkalmazásainak lehetőségei; PREGA SCIENCE'20, Precíziós Gazdálkodási Konferencia (2020. február 18.)

VARGA ZS. (2022): Flood susceptibility mapping in Hungary based on remote sensed images and machine learning methods, *GeoMATES '22; International Congress on Geomathematics in Earth- & Environmental Sciences (2022.05.19-21.)*